

Power Control Strategies in C+L Optical Line Systems

Original

Power Control Strategies in C+L Optical Line Systems / Ferrari, Alessio; Pileri, Dario; Virgillito, Emanuele; Curri, Vittorio. - ELETTRONICO. - W2A.48:(2019), pp. 1-3. (Intervento presentato al convegno Optical Fiber Communication Conference (OFC) tenutosi a San Diego CA (USA) nel 3–7 March 2019) [10.1364/OFC.2019.W2A.48].

Availability:

This version is available at: 11583/2734312 since: 2019-05-29T08:35:11Z

Publisher:

OSA

Published

DOI:10.1364/OFC.2019.W2A.48

Terms of use:

This article is made available under terms and conditions as specified in the corresponding bibliographic description in the repository

Publisher copyright

Optica Publishing Group (formely OSA) postprint/Author's Accepted Manuscript

“© 2019 Optica Publishing Group. One print or electronic copy may be made for personal use only. Systematic reproduction and distribution, duplication of any material in this paper for a fee or for commercial purposes, or modifications of the content of this paper are prohibited.”

(Article begins on next page)

Power Control Strategies in C+L Optical Line Systems

Alessio Ferrari, Dario Piloni, Emanuele Virgillito and Vittorio Curri

DET, Politecnico di Torino, C.so Duca degli Abruzzi 24, 10129 Torino, Italy. alessio.ferrari@polito.it

Abstract: Following the LOGO paradigm, we propose and test frequency-dependent power control strategies and show that 50% pre-tilting for the L-band and flat launch for the C-band is a good strategy as predicted by the GGN-model.

OCIS codes: (060.2330) Fiber optics communications; (060.1660) Coherent communications;

1. Introduction

5G access and cloud computing will drive a dramatic increase in IP traffic over the next years [1]. Contrary to access networks, backbone networks are already carrying massive amount of data and will be required to push further the capacity by exploiting the existing infrastructure, as operators aim at maximizing their returns on CAPEX. The low loss transmission bandwidth of the optical fiber is much larger than the presently used 5 THz of the C-band, and it is as large as 50 THz in modern standard single mode fibers (SSMF) with reduced absorption water-peak. Also, optical amplifiers (OAs) are now commercially available for bands beyond the C-band, starting from the L-band. So, multiband transmission has been proposed, and C+L optical line systems (OLS) are already implemented [2]. Besides the availability of the HW equipment, the upgrade to multiband transmission requires the implementation of OLS SW controllers able to fully exploit the fiber capacity. In state-of-the-art networks, it has been extensively demonstrated that the unique quality-of-transmission (QoT) figure is the signal-to-noise ratio (SNR) determining the BER, independently of the transponder vendor [3]. The SNR is given by the effect of the OA ASE noise and of the non-linear interference (NLI) disturbance generated by nonlinear fiber propagation that increases with power. Thus, for every deployed lightpath (LP), there exists an optimal power maximizing the SNR and consequently the transmission capacity: power controlling is so the key-operation within the OLS controller. As both the ASE noise and the NLI can be assumed to accumulate incoherently with the amplified OLS spans, the local-optimization global-optimization (LOGO) [5] strategy has been proposed to set the optimal power. For the C-band, the LOGO implementation is based on neglecting any frequency dependence and focuses on the worst-case channel at the bandwidth center, for which the optimal power is set using the GN-model for NLI calculation. Such an approach has proved to be practical effective for C-band OLSs, while it becomes progressively suboptimal when filling the entire C-band and beyond. Specifically, the bandwidth extension is triggering more intensely the stimulated Raman scattering (SRS) that is maximally intense over a bandwidth of 13 THz [6-11]. Moreover, the application of distributed Raman amplification (DRA), and in general the ASE noise dependence on the frequency, require a frequency-dependent approach to avoid the introduction of large system margins. On one side, such an approach requires a detailed knowledge of frequency-dependent characteristics of network elements, specifically for fiber and OA parameters. And this is a request to be fulfilled by the capability to properly get parameters from installed equipment. On the other side, the NLI generation must also consider the wide-band effects, and in particular the interaction of NLI generation with frequency variations of the power profile, mostly induced by SRS and DRA. To this purpose, the generalized GN (GGN) model has been proposed [6-9] and experimentally validated [10,11]. Like the GN-, the GGN-model has proved to be accurate yet conservative in predicting the NLI [10]. In this work, we follow the LOGO paradigm overcoming the frequency independence and proposing different power control strategies to maximize transmission capacity on C+L OLSs. We assume to be able to implement a different average power level and linear pre-tilting on the C- and L-band and consider four different strategies tested by simulation [12] on a 10-span OLS operated by 200G PM-16QAM channels. We show that the strategy implying pre-tilting of 50% of SRS+DRA effects in L-band and flat transmitted power in the C-band is a practical engineering rule to be implemented in C+L power controlling to get uniform QoT over the entire C+L band.

2. Analysis

We consider the physical layout depicted in Figs. 1 and 2. The OLS is loaded by 161 32-GBaud PM-16QAM (200G) transmitters on both the C- and L-band, generating WDM channel combs filling both the bands. The C-band channels are 83, and L-band channels are 78. We assume to operate on the 50 GHz DWDM grid, keeping a 250 GHz guard-band between the two bands. The two combs are then multiplexed, and the overall spectrum is transmitted over a 10-span OLS. Each span consists of 80 km of SSMF, followed by a hybrid fiber amplifier (HFA) composed by a backward-pumping Raman amplifier module, followed by a lumped erbium doped fiber amplifier (EDFA). We assume a DRA enabled by 5 pumps configured as reported in Tab. 1, following by an EDFA with a Gain Flattening Filter (GFF) that recovers for the remaining loss and flattens the spectrum. At the receiver, channels are detected by typical DSP-based coherent receivers. Due to the intense SRS effect on each span, we realistically suppose the C- and L-band combs are spectrally separated at the end of each amplified span to independently apply two different

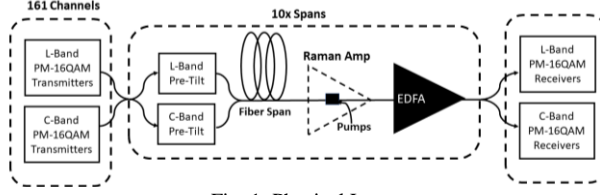


Fig. 1: Physical Layout

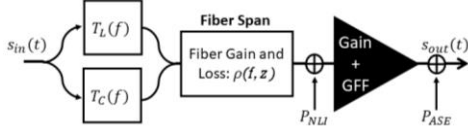


Fig. 2: Equivalent block scheme of one span

| Pump # | Frequency | Power |
|--------|------------|--------|
| 1 | 200.27 THz | 150 mW |
| 2 | 201.61 THz | 250 mW |
| 3 | 207.18 THz | 150 mW |
| 4 | 208.62 THz | 250 mW |
| 5 | 210.08 THz | 200 mW |

Table 1: Power and frequency of the five pumps composing the Raman amplifier

spectral tilting: $T_C(f)$ and $T_L(f)$, for the C- and the L-band, respectively. The two spectral portions are then recombined and launched in the following span. The system is thus strictly periodical and the spectrum at the input of each fiber span has always the same shape. Therefore, each span may be modeled by the equivalent linear block-diagram of Fig. 2. Spectral tilting modules are linear filters, fiber is described by its gain-and-loss profile $\rho(f, z)$ taking into account both frequency-dependent attenuation and the SRS+DRA effects. The effects of nonlinear fiber propagation are considered by the NLI adding after the application of $\rho(f, z)$; the NLI power P_{NLI} in each signal slot is computed by the GGN-model [7]. After the NLI adding-point, the equivalent block diagram includes the block considering the EDFA which includes an ideal GFF that flattens the spectrum. Then, the overall equivalent ASE noise generated by optical amplification is added. Since the power spectral density (PSD) of the equivalent ASE noise depends on the specific implementation of the HFA, we suppose a flat PSD to keeping the obtained results agnostic with respect to the HFA implementations. So, the overall noise figure of the HFA is frequency-independent, and we set it to 1.6 dB. On the described system, we tested different power control strategies by applying different tilting on the C- and L-band at the beginning of each span. For each tested strategy, we keep the power at the center of the C+L overall bandwidth at the GN-model-predicted optimal value and we independently tilt the two bands (C and L). First, we considered the simplest method as a reference: on both bands the launched power spectral density (PSD) is set flat at the GN-model-predicted optimal power [13] (0/0 strategy). The second heuristic we tested was the application of a single overall tilt on the entire C+L band to completely pre-compensate the total spectral tilt induced by the fiber gain-and-loss profile $\rho(f, z)$ (100/100 strategy). The third strategy is similar to the second one, but only 50% of the $\rho(f, z)$ tilt is pre-compensated (50/50 strategy). These are typical strategies commonly used in single C-band transmission. Then, we investigated on better power management techniques, searching for the tilting on the two bands that maximizes and equalizes the channel QoTs on the overall bandwidth, i.e., the SNR for each channel:

$$\text{SNR} = \frac{P_S}{P_{ASE} + P_{NLI}} = \frac{1}{\text{OSNR}^{-1} + \text{SNR}_{NL}^{-1}}, \quad (1)$$

where the optical signal to noise ratio (OSNR) considers only the ASE noise, and the non-linear signal to noise ratio (SNR_{NL}) summarizes the effects of fiber nonlinear propagation and consequent NLI generation. To derive engineering rules to apply separately on the C- and L-band, we aimed at evaluating Eq. (1) exploring all the tilting possibilities. To this purpose, it was not possible to run split-step simulations because of the large computational time. Therefore, we relied on the GGN-model, with the knowledge that it considers the interaction of NLI generation with the fiber gain-and-loss profile and it is conservative in predicting the NLI intensity over the entire bandwidth. We varied the C- and L-band pre-tilting between 0% and 200% of the of the $\rho(f, z)$ as shown in Fig. 3a, resulting on the SNR evaluations displayed in Fig. 3b. Among all results, we chose the one equalizing the SNR on both bandwidths; so, we decided to test as fourth strategy 50% pre-compensation in the L-band and 0% in the C-band (50/0 strategy).

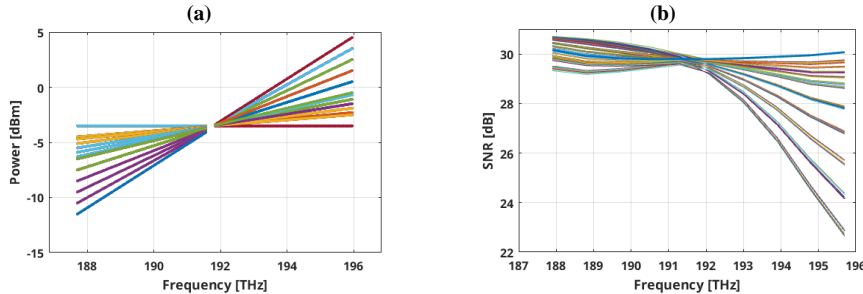


Fig. 3: Tilting strategies as at the span inlets (a) and the corresponding SNR curves after one span propagation (b)

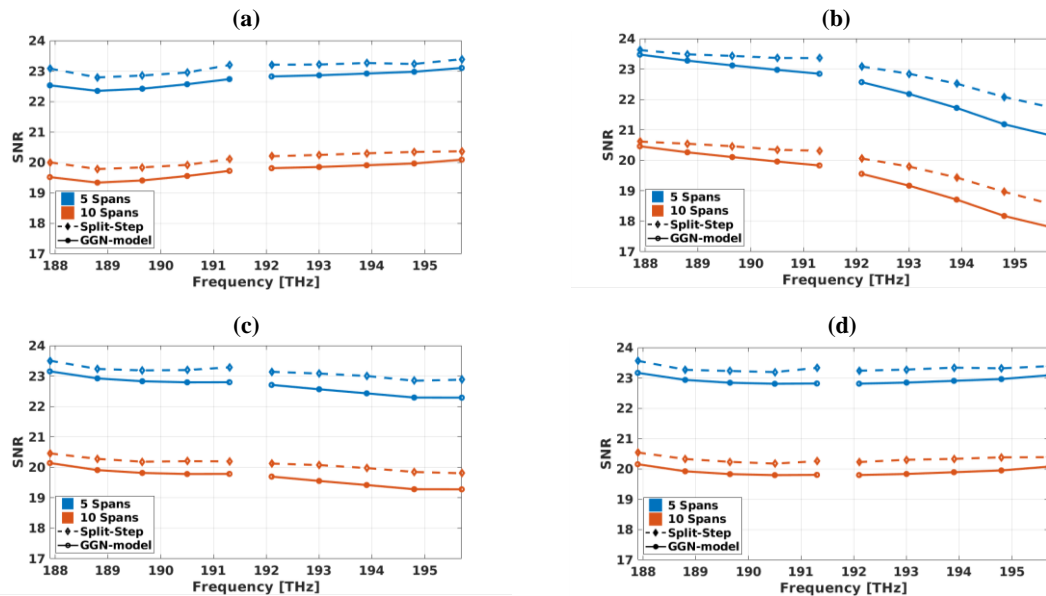


Fig. 4: QoT performances using (a) 0/0 strategy, (b) 100/100 strategy, (c) 50/50 strategy, (d) 50/0 strategy.

3. Simulative validation

To compare the effectiveness of the four proposed strategies, we performed full time-domain split-step simulations using the FFSS library [12] over the same scenario previously described. The channels under test (CUTs) for which we computed the SNR are 10 – 5 for each band – at the frequencies: 187.9 THz, 188.8 THz, 189.65 THz, 190.5 THz, 191.3 THz, 192.1 THz, 193.0 THz, 193.9 THz, 194.8 THz and 195.7 THz. The GN-model-based optimal power per channel [13] is equal to -3.5 dBm, and the overall fiber tilt is ~8 dB. Simulation results are plotted as SNR vs. frequency in Figs. 4 for 5 spans propagation (blue lines) and 10 spans propagation (red lines). Dashed lines refer to simulative results, while GGN-model results are plotted as a comparison as continuous lines. The four figures refer to the four considered tilting strategies. In general, we can observe that the GGN-model is confirmed to be an excellent analytical tool for accurate yet conservative QoT estimation over multi-band transmission. The other general comment is on the incoherent accumulation of disturbances with spans, confirmed by the exact 3 dB difference between SNR results for 5 and 10 spans. Comparing the different strategies, we note that the 0/0 strategy is largely suboptimal, especially in the L-band, where the SNR is lower. Then, if a pre-emphasis is applied to totally compensate the tilt introduced by the fiber (100/100 strategy, Fig. 4.b), L-band performance improves but, in the C-band, the SNR decreases significantly. In this case, the overall SNR unbalancing is ~2 dB. Then, as a trade-off between the first two heuristics the 50/50 strategy results are shown in Fig. 4.c. In this case, the overall performance is better than before, but there is still a large unbalancing in the performances between C and L bands. Finally, observing Fig. 4d, we note that the proposed 50/0 strategy presents a very good balance between C-band and L-band performances, displaying a practically flat SNR curve, and so proving to be the best option to setting launch power in C+L-band OLSs.

4. Comments and conclusions

We showed that approaching the power control of multi-band OLSs as typically is done for a single-band usage is always suboptimal. Keeping the pivotal power at the center of the C+L bandwidths and unlocking the pre-tilting slope applied to the two bandwidths, we exploited the GGN-model to define a practical strategy aimed at equalizing the overall QoT on both C- and L-band. It resulted that the 50/0 strategy was the better choice. We tested the strategy by simulation and confirmed that the overall SNR is practically flat on the entire C+L band, after the propagation over a 10-span optical line system relying on hybrid EDFA/Raman amplification.

References

- [1] Forecast, Cisco VNI. "Cisco visual networking index: VNI Global Fixed and Mobile Internet Traffic Forecasts 2016-2021." CISCO, 2018.
- [2] http://photonics-complete.eu/wp-content/uploads/2018/01/trends_in_optical_disagg_lr_webinar_.pdf
- [3] M. Filer et al. "Multi-Vendor Experimental Validation of an Open Source QoT Estimator for Optical Networks", JLT, 2018.
- [4] P. Poggiolini et al., "The GN-Model of Fiber Non-Linear Propagation and its Applications", JLT, 2014.
- [5] P. Poggiolini et al., "The LOGON Strategy for Low-Complexity Control Plane Implementation...", OFC, 2013.
- [6] M. Cantono et al., "Introducing the Generalized GN-model for Nonlinear Interference ...", arXiv preprint arXiv:1710.02225, 2017.
- [7] M. Cantono et al., "Modelling the Impact of SRS on NLI Generation in Commercial Equipment: an Experimental ...", OFC, 2018.
- [8] I. Roberts et al., "Channel Power Optimization of WDM Systems Following...", JLT, 2017.
- [9] D. Semrau et al., "The Gaussian noise model in the presence of inter-channel stimulated Raman scattering," JLT, 2018.
- [10] M. Cantono et al., "On the Interplay of Nonlinear Interference Generation with Stimulated Raman Scattering ...", JLT, 2018.
- [11] M. Cantono et al., "Physical Layer Performance of Multi-Band Optical Line Systems Using Raman Amplification", JOCN, 2018.
- [12] D. Pileri, et al., "FFSS: The fast fiber simulator software", ICTON, 2017.
- [13] V. Curri et al., "Design Strategies and Merit of System Parameters for Uniform Uncompensated...", JLT, 2015